

# Thickness Reduction Controller Design for Flying Gauge Change in a Cold Strip Mill

Tomoyoshi Ogasahara

Instrument and Control Engineering Research Dept.  
JFE Steel Corp.,  
1 Kokan-cho, Fukuyama, Hiroshima, Japan  
t-ogasahara@jfe-steel.co.jp

**Abstract**—This paper proposes a new flying gauge change (FGC) scheme for a continuous cold strip mill to achieve thickness reduction in a specified section including a welding point. Because this section is often processed as scrap, thickness reduction is desired as a means of reducing scrap weight. However, this is not possible with conventional FGC, which considers only one thickness change point, because two thickness change points exist simultaneously in the mill due to the short length of the specified section. The proposed scheme utilizes the transition pattern of the position of the two thickness change points during FGC to calculate the set values of the roll gap and roll speed. Thickness reduction is achieved by applying these set values to the rolling mill according to the tracking signals of the two thickness change points. The validity of the proposed method was verified by simulation and experiments. Application of this technology has improved cold strip yield.

**Keywords**—control; flying gauge change; cold rolling; physical model; actuator model; model based design.

## I. INTRODUCTION

In a continuous cold strip mill, as shown in Figure 1, a coil is uncoiled by the pay-off reel, and its lead end is welded to the tail end of the preceding strip. Here, the two strips differ in hardness and dimensions, such as thickness and width, and the specified thickness after rolling also differs. Hence, the rolling mill must change the thickness of the strip at the welding point. After rolling, the strips are cut at the welds and coiled separately by the tension reel. Flying Gauge Change (FGC) was developed in order to achieve the necessary thickness change [1][2][3]. Although the most important issue in FGC is obviously thickness accuracy, it is also necessary to minimize strip tension deviations in order to prevent rolling trouble such as strip breakage. In Yamashita et al. [1], the responses of the actuators, which consist of the roll gap and roll speed, are synchronized during FGC, thereby minimizing strip tension deviations. In [2], the set values of the roll gap and speed are also synchronized. Furthermore, a dynamic setup model based on the measured value of strip thickness is proposed to compensate for setup model error. Hol et al. [3] explicitly introduces strip tension and thickness to the controller objective function and directly optimizes the time-domain response, and the inherent variation of the forward slip and friction conditions is mentioned.

On the other hand, a specified section including a welding point is often processed as scrap due to the mechanical properties of the strip or constraints of the downstream manufacturing processes. Therefore, as shown in Figure 2, thickness reduction in that section is desired as a means of reducing scrap weight, and thereby, improving yield. FGC must be applied in order to achieve this thickness reduction in a cold rolling mill. However, thickness reduction is not possible with the conventional FGC method, which considers only one thickness change point, because two thickness change points exist simultaneously in the mill due to the short length of the specified section. Figure 3 shows this situation.

This paper presents a new FGC method which makes it possible to achieve the prescribed two thickness changes. To simplify the problem, the size and hardness of the welded preceding and succeeding strips are the same. While this situation often occurs in actual operation, this can also be eliminated by a few modifications to the technology presented in this paper.

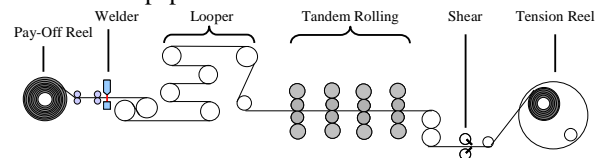


Figure 1. Outline of a Cold Strip Mill

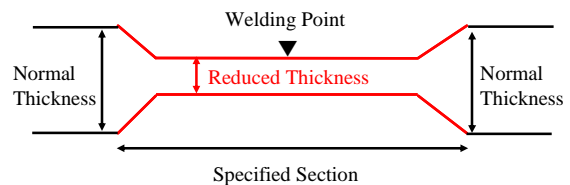


Figure 2. Thickness Reduction for Yield Improvement

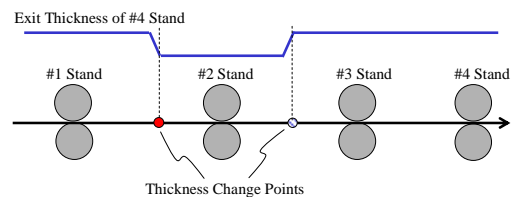


Figure 3. Two Thickness Change Points in the Mill

The outline of this paper is as follows. In Section II, a dynamical model and the principle of the conventional FGC are shown. In Section III, the details of the proposed FGC algorithm are explained. In Section IV, simulation and experimental results are presented. Finally, the conclusions are summarized in Section V.

II. DYNAMICAL MODEL OF A COLD STRIP MILL AND A CONVENTIONAL FGC METHOD

A dynamical model of a cold strip mill and a conventional FGC method are explained in this section. The model is used in designing the FGC controller.

A. Dynamical model of a cold strip mill

The model consists of physical models and actuator models. Each model is shown below, and the variables in the models are summarized at TABLE I. Note that the suffix  $i$  in the variables indicates the  $i^{th}$  stand.

- Rolling Force

$$P_i = wk_i K_t \sqrt{R'_i(H_i - h_i)} Q_i.$$

where,

$$K_t = (1 - \sigma_{bi} / k_i) \left( 1.05 + 0.1 \frac{1 - \sigma_{fi} / k_i}{1 - \sigma_{bi} / k_i} - 0.15 \frac{1 - \sigma_{bi} / k_i}{1 - \sigma_{fi} / k_i} \right),$$

$$R'_i = R_i \left( 1 + \frac{16(1 - \nu^2)}{E\pi} \frac{P_i}{w(H_i - h_i)} \right),$$

$$Q_i = 1.08 + 1.79r_i\mu_i \sqrt{\frac{R'_i}{H_i}} - 1.02r_i.$$

- Forward Slip Model

$$f_i = \tan^2 \left( \frac{1}{2} \arctan \left( \sqrt{\frac{r_i}{1 - r_i}} \right) - \frac{1}{4\mu_i} \log \left( \frac{H_i}{h_i} \frac{1 - \sigma_{fi} / k_{fi}}{1 - \sigma_{bi} / k_{bi}} \right) \sqrt{\frac{h_i}{R'_i}} \right).$$

- Strip Tension Model

$$T_{i-i+1} = \frac{E}{L} \int (V_{i+1} - v_i) dt. \tag{1}$$

- Thickness Model

$$h_i = S_i + P_i / M_i. \tag{2}$$

- Roll Speed Actuator Model

$$V_{Ri}(s) = \frac{1}{T_i^v s + 1} V_{Ri}^{ref}(s). \tag{3}$$

- Roll Gap Position Actuator Model

$$S_i(s) = \frac{1}{T_i^s s + 1} S_i^{ref}(s). \tag{4}$$

- Transport Delay Model

$$H_{i+1} = h_i \exp(-L / v_i s). \tag{5}$$

- Conservation Law of Mass Flow

$$V_i H_i = v_i h_i. \tag{6}$$

In these models, rolling force and forward slip can be calculated according to the models in [4][5]. The strip

tension between the  $i^{th}$  stand and  $i+1^{th}$  stand is represented as (1). This model means that strip tension fluctuates when the velocity of the entry strip at the  $i+1^{th}$  stand differs from that of the exit strip at the  $i^{th}$  stand. This is an important characteristic for FGC. In the thickness model shown in (2), thickness is determined by the roll gap  $S_i$  and elastic deformation of a work roll, which is represented as  $P_i / M_i$ . The actuators of the mill are electric motors and hydraulic cylinders. The former are for controlling the roll speed, and the latter for controlling the roll gap position. These actuators can be modeled as first order transfer functions like (3) and (4). The transport time delay is variable, depending on the strip velocity, and is modeled as (5). The conservation law of mass flow is described as (6).

TABLE I. PARAMETERS IN THE MODEL

Symbol	Notes
$P_i$	Rolling force
$w$	Strip width
$k_i$	Mean deformation resistance
$k_{bi}$	Entry deformation resistance
$k_{fi}$	Exit deformation resistance
$K_t$	Tension correction term
$R'_i$	Flattened work roll radius
$H_i$	Entry thickness
$h_i$	Exit thickness
$Q_i$	Influence of friction coefficient
$\sigma_{bi}$	Unit tension of entry side of a stand
$\sigma_{fi}$	Unit tension of exit side of a stand
$r_i$	Reduction rate
$\mu_i$	Friction coefficient
$\nu$	Poisson's ratio of work roll
$f_i$	Forward slip
$T_{i-i+1}$	Strip tension between $i^{th}$ stand and $(i+1)^{th}$ stand
$E$	Young's modulus
$L$	Length between stands
$V_i$	Entry strip velocity; $V_{Ri}(f_i + 1)h_i / H_i$
$v_i$	Exit strip velocity; $V_{Ri}(f_i)$
$S_i$	Roll gap
$M_i$	Mill modulus
$s$	Laplace operator
$V_{Ri}$	Roll speed
$V_{Ri}^{ref}$	Reference of roll speed
$T_i^v$	Time constant of roll speed actuator
$S_i^{ref}$	Reference of roll gap position
$T_i^s$	Time constant of roll gap position actuator

B. Conventional FGC method

The conventional FGC method is explained here. Figure 4 shows an example of the time chart of the action of the actuators during FGC. The roll gap is being closed when the thickness change point passes each of the stands. On the other hand, the roll speed of the  $i^{th}$  stand does not decrease when the point passes the  $i^{th}$  stand, but decreases when the point passes the  $i+1^{th}$  stand. The reason for this can be explained by (1) and (6). From (6), we obtain

$$V_{i+1} = v_{i+1}h_{i+1} / H_{i+1} \tag{7}$$

Because  $h_{i+1}$  becomes smaller by closing the roll gap,  $V_{i+1}$  in (7) also becomes smaller. To minimize the deviation of strip tension,  $v_i = V_{i+1}$  is required from (1). For this, it is necessary to decrease the speed of the  $i^{th}$  stand. Synchronization of the responses of the roll gap and speed to minimize the imbalance of the mass flow during the transition period is described in [1].

In order to calculate the strip velocity during FGC, information on the thickness and initial strip velocity are required. The reference thickness after FGC is determined by the setup calculation of the mill, and the initial strip velocity is usually estimated by  $V_{Ri}(f_i + 1)$ . Finally, the roll speed during FGC is calculated by using the prescribed strip velocity and forward slip after FGC based on the forward slip model. The roll gap is calculated by (2).

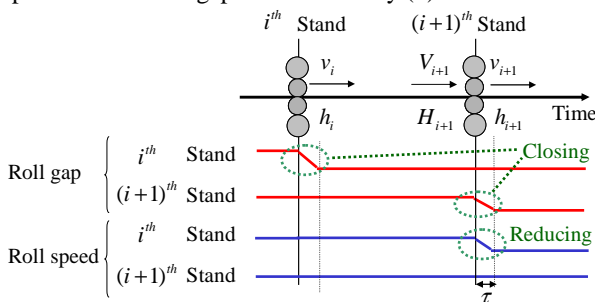


Figure 4. Time Chart of the Action of Actuators during FGC

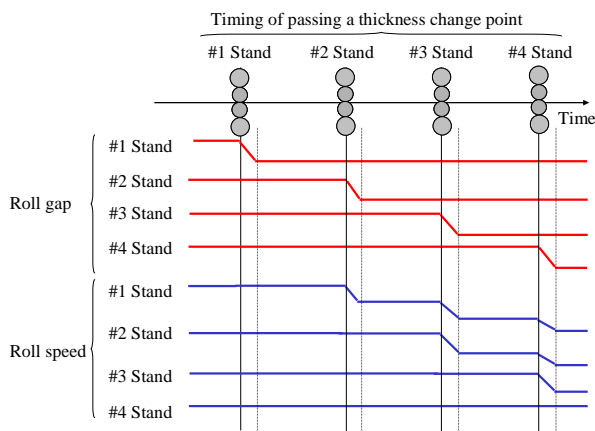


Figure 5. FGC Time Chart of a Conventional Method

FGC is achieved by applying these set values to the rolling mill according to the tracking signal of the thickness change point. This situation is shown in Figure 5. The above is the outline of the conventional method.

III. THICKNESS REDUCTION CONTROLLER DESIGN

The thickness reduction controller design is presented in this section. The proposed method consists of three steps. The 1st step is to classify the transition pattern of the position of the two thickness change points during the FGC. The 2nd step is to calculate the set values of the roll gap and the roll speed based on the results of the 1st step. The 3rd step is to apply these set values to the rolling mill according to the tracking signals of the two thickness change points.

A. Classification of the transition pattern

The volume of the specified section between two thickness change points is invariant. Based on this fact, the transition pattern of the position of the two thickness points can be classified under several cases. Here,  $A$  denotes the first thickness change point,  $B$  denotes the second thickness change point,  $M$  is the volume of the specified section and  $h_i^{II}$  is the reference of the exit thickness of the  $i^{th}$  stand of the specified section.

Let us consider the pattern shown in Figure 6. Firstly,  $A$  exists between No. 1 stand and No. 2 stand in state-1. Then,  $A$  moves to between No. 2 stand and No. 3 stand in the following state-2. Because  $M$  is larger than  $h_1^{II} \times L$ ,  $B$  cannot enter between No. 1 stand and No. 2 stand at that time. In the following state-3,  $B$  enters between No. 1 stand and No. 2 stand because  $M$  is smaller than  $(h_1^{II} + h_2^{II}) \times L$ . State-4 shows that  $A$  moves to between No. 3 stand and No. 4 stand. The reason for this is explained as follows: When state-1 exists, the inequality  $h_2^{II} \times L \leq h_1^{II} \times L \leq M$  is obtained. Thus,  $B$  cannot enter between No. 2 stand and No. 3 stand in this state. In the following state-5,  $B$  enters between No. 2 stand and No. 3 stand since  $M$  is smaller than  $(h_2^{II} + h_3^{II}) \times L$ . The following state-6, state-7, and state-8 are obvious. Thus, the transition pattern is classified based on the volume of the specified section.

A summary of the transition pattern is shown in Figure 7. The transition pattern is classified under four cases. The subscripts to  $A$  and  $B$  indicate that the thickness change point passes the stand indicated by the numbers.

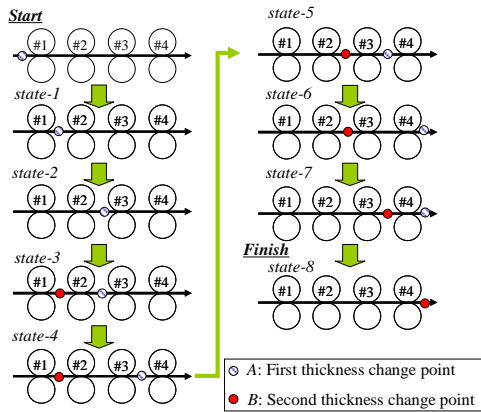


Figure 6. An Example of a Transition Pattern of the Position of the Two Thickness Change Points

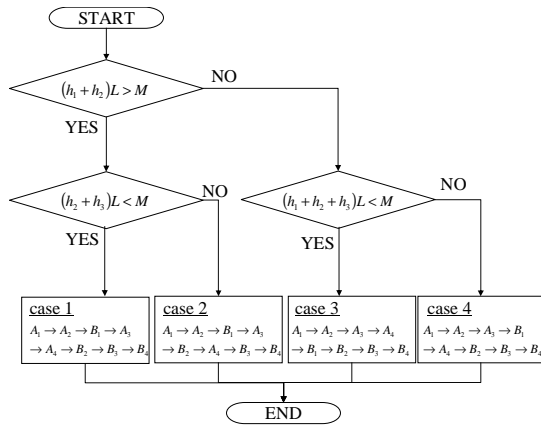


Figure 7. The Logic of Classifying the Transition Pattern

**B. Calculation of the set values of the roll gaps and the roll speed**

The set values of the roll gap and the roll speed must be changed to achieve thickness reduction when the thickness change points pass each stand. As is described in Section II, the roll gap can be obtained by (1) and the roll speed can be calculated from the thickness information and the forward slip and initial roll speed. Classification of the pattern is performed in order to obtain the thickness information when the thickness change points pass each stand.

An example of a state for roll speed calculation is shown in Figure 8. Here,  $h_i^I$  denotes the initial exit thickness of the  $i^{th}$  stand and  $h_i^{II}$  means the reduced exit thickness of the  $i^{th}$  stand. The roll speed of the final stand, described as  $V_{R4}^I$ , is fixed. The variables,  $V_{R1}^*$ ,  $V_{R2}^*$  and  $V_{R3}^*$  must be calculated.  $f_i^I$  is the forward slip of the  $i^{th}$  stand in the initial rolling condition, and  $f_i^{II}$  is the forward slip of the  $i^{th}$  stand in the reduced thickness rolling condition. The calculation is executed as follows.

From the conservation of mass flow in No. 4 stand, we obtain  $V_{R3}^*(1 + f_3^{II})h_3^I = V_{R4}^I(1 + f_4^I)h_4^I$ . This formula is deformed as

$$V_{R3}^* = V_{R4}^I \frac{1 + f_4^I}{1 + f_3^{II}} \frac{h_4^I}{h_3^I} \quad (8)$$

We obtain  $V_{R2}^*(1 + f_2^{II})h_2^{II} = V_{R3}^*(1 + f_3^{II})h_3^{II}$  from the conservation of mass flow in No. 3 stand. By using (8), this formula is deformed as

$$V_{R2}^* = V_{R3}^* \frac{1 + f_3^{II}}{1 + f_2^{II}} \frac{h_3^{II}}{h_2^{II}} = V_{R4}^I \frac{1 + f_4^I}{1 + f_2^{II}} \frac{h_4^I}{h_3^I} \frac{h_3^{II}}{h_2^{II}} \quad (9)$$

From the conservation of mass flow in No. 2 stand, we obtain  $V_{R1}^*(1 + f_1^I)h_1^{II} = V_{R2}^*(1 + f_2^{II})h_2^{II}$ . This formula is deformed as

$$V_{R1}^* = V_{R2}^* \frac{1 + f_2^{II}}{1 + f_1^I} \frac{h_2^{II}}{h_1^{II}} = V_{R4}^I \frac{1 + f_4^I}{1 + f_1^I} \frac{h_4^I}{h_3^I} \frac{h_3^{II}}{h_1^{II}} \quad (10)$$

Thus, the set values of roll speed are obtained as (8), (9) and (10). The roll speed should be obtained for all states. The results are shown in TABLE II.

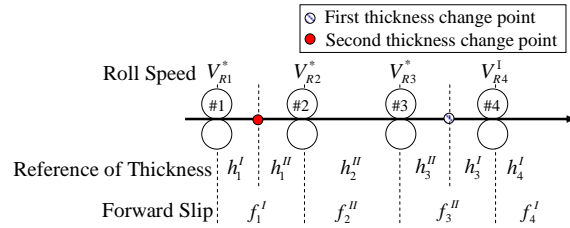


Figure 8. An Example of a State for Roll Speed Calculation

TABLE II. ROLL SPEED SETTINGS

State	$V_{R1}^*$	$V_{R2}^*$	$V_{R3}^*$
1	$V_{R4}^I \frac{1 + f_4^I}{1 + f_1^I} \frac{h_4^I}{h_1^I}$	$V_{R4}^I \frac{1 + f_4^I}{1 + f_2^{II}} \frac{h_4^I}{h_2^{II}}$	$V_{R4}^I \frac{1 + f_4^I}{1 + f_3^{II}} \frac{h_4^I}{h_3^I}$
2	$V_{R4}^I \frac{1 + f_4^I}{1 + f_1^I} \frac{h_4^I}{h_1^{II}} \frac{h_2^{II}}{h_1^{II}}$	$V_{R4}^I \frac{1 + f_4^I}{1 + f_2^{II}} \frac{h_4^I}{h_2^{II}}$	$V_{R4}^I \frac{1 + f_4^I}{1 + f_3^{II}} \frac{h_4^I}{h_3^I}$
3	$V_{R4}^I \frac{1 + f_4^I}{1 + f_1^I} \frac{h_4^I}{h_1^I} \frac{h_2^{II}}{h_2^I}$	$V_{R4}^I \frac{1 + f_4^I}{1 + f_2^{II}} \frac{h_4^I}{h_2^{II}}$	$V_{R4}^I \frac{1 + f_4^I}{1 + f_3^{II}} \frac{h_4^I}{h_3^I}$
4	$V_{R4}^I \frac{1 + f_4^I}{1 + f_1^I} \frac{h_4^I}{h_3^I} \frac{h_3^{II}}{h_1^{II}}$	$V_{R4}^I \frac{1 + f_4^I}{1 + f_2^{II}} \frac{h_4^I}{h_3^I} \frac{h_3^{II}}{h_2^{II}}$	$V_{R4}^I \frac{1 + f_4^I}{1 + f_3^{II}} \frac{h_4^I}{h_3^I}$
5	$V_{R4}^I \frac{1 + f_4^I}{1 + f_1^I} \frac{h_4^I}{h_3^I} \frac{h_3^{II}}{h_2^I} \frac{h_2^{II}}{h_1^{II}}$	$V_{R4}^I \frac{1 + f_4^I}{1 + f_2^{II}} \frac{h_4^I}{h_3^I} \frac{h_3^{II}}{h_2^{II}}$	$V_{R4}^I \frac{1 + f_4^I}{1 + f_3^{II}} \frac{h_4^I}{h_3^I}$
6	$V_{R4}^I \frac{1 + f_4^I}{1 + f_1^I} \frac{h_4^I}{h_2^I} \frac{h_2^{II}}{h_1^I}$	$V_{R4}^I \frac{1 + f_4^I}{1 + f_2^{II}} \frac{h_4^I}{h_2^{II}}$	$V_{R4}^I \frac{1 + f_4^I}{1 + f_3^{II}} \frac{h_4^I}{h_3^I}$
7	$V_{R4}^I \frac{1 + f_4^I}{1 + f_1^I} \frac{h_4^I}{h_3^I} \frac{h_3^{II}}{h_1^I}$	$V_{R4}^I \frac{1 + f_4^I}{1 + f_2^{II}} \frac{h_4^I}{h_3^I} \frac{h_3^{II}}{h_2^I}$	$V_{R4}^I \frac{1 + f_4^I}{1 + f_3^{II}} \frac{h_4^I}{h_3^I}$
8	$V_{R4}^I \frac{1 + f_4^I}{1 + f_1^I} \frac{h_4^I}{h_1^I}$	$V_{R4}^I \frac{1 + f_4^I}{1 + f_2^{II}} \frac{h_4^I}{h_2^I}$	$V_{R4}^I \frac{1 + f_4^I}{1 + f_3^{II}} \frac{h_4^I}{h_3^I}$

C. Applying the set values to the mill

Thickness reduction is achieved by applying the set values to the rolling mill according to the tracking signals of the two thickness change points. The control system is shown in Figure 9. The state can be judged by the tracking signals, and the appropriate set values are selected. The set values are then sent to the mill controller, and the roll gap and roll speed are controlled.

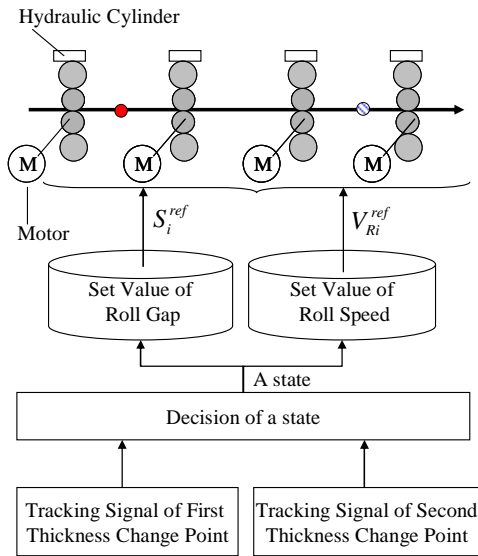


Figure 9. The Proposed Control System

The procedure outlined above is the proposed method.

IV. SIMULATION AND EXPERIMENTS

The results of a simulation and experiments are presented here. In the chart graph of the simulation and experiments, the value on the vertical axis is normalized by the initial value, which is the value before applying thickness reduction control.

A. Simulation

Figures 10 and 11 show the actions of the roll gap and roll speed, respectively. In Figure 10, the roll gap is being closed when the first thickness change point passes each stand, and it is being opened when the second thickness change point passes each stand. Thus, the action of the roll gap is simple and the existence of the two thickness change points in the mill is confirmed by the graph. The action of the roll speed, especially at No. 1 stand in Figure 11, is somewhat complex. It was found that the effect of the two thickness change points appears in the upstream stand speed. The strip tension will deviate unless the roll speed is set appropriately.

Figure 12 shows the strip tension deviations. In order to maintain unit tension, which is the tension per cross sectional area of the strip, the set value of tension is decreased. Strip deviation is within 20% in this graph. In actual operation, strip tension deviation within 30% is desired in order to

prevent rolling trouble. Hence, this method achieves tension deviation within the reference value.

Figure 13 is a thickness chart. A thickness reduction of nearly 50% is achieved by using the proposed method.

Thus, these simulation results verify the validity of the proposed method from the viewpoints of thickness and strip tension deviations.

B. Experimental results

The experimental results are shown in Figure 14 and Figure 15. In this control method, the reference of thickness reduction is 11% compared to the thickness before application. Strip tension deviation within 10% was obtained in this experiment. Hence, this method satisfies the condition for actual operation. Thickness fluctuated at the welding point at 19 [sec] due to the difference of the deformation resistance of the welded strips.

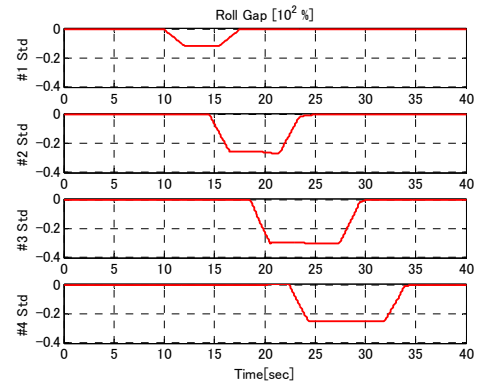


Figure 10. Roll Gap (Simulation)

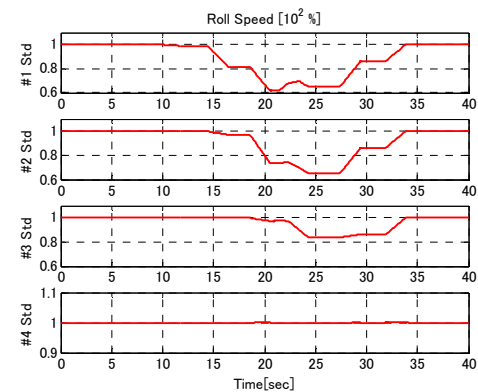


Figure 11. Roll Speed (Simulation)

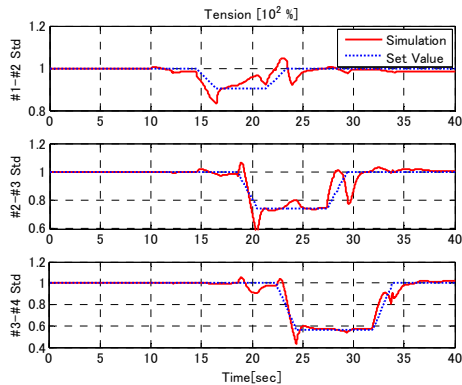


Figure 12. Strip Tension (Simulation)

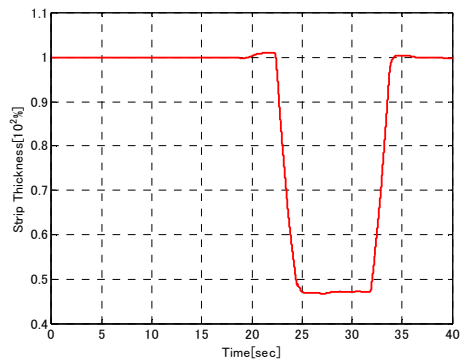


Figure 13. Exit Thickness of Final Stand (Simulation)

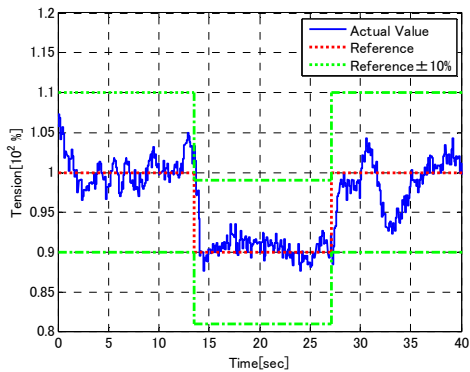


Figure 14. Strip Tension between No. 3 Stand and No. 4 Stand (Experiment)

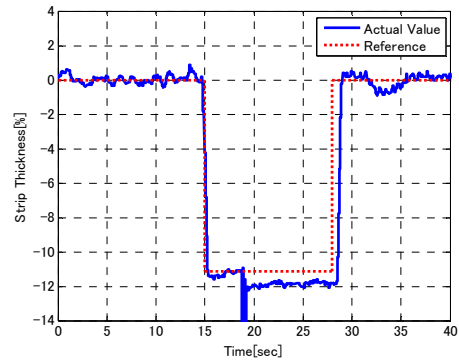


Figure 15. Exit Thickness of Final Stand (Experiment)

However, in total, thickness accuracy is controlled to within 1%, demonstrating accurate thickness control. Thus, the validity of this method was also verified experimentally.

### V. CONCLUSIONS

In a continuous cold strip mill, a specified section including a welding point is often processed as scrap. In order to reduce scrap weight and improve product yield, reduction of the thickness of this section is desired.

A new FGC method which achieves two thickness changes is proposed in this paper. The proposed method classifies the transition pattern of the two thickness change points in the mill and calculates the set values of the roll gap and the roll speed, thereby simultaneously achieving the desired thickness reduction and reducing tension deviations.

In a simulation, a thickness reduction of nearly 50% and strip deviation within 20% were obtained. Experimental results also showed that thickness reduction and low tension deviation are achieved by this FGC method.

Thus, the validity of the proposed method was verified by both simulation and experiments. Application of this technology has resulted in improved cold strip yield.

### REFERENCES

- [1] M. Yamashita, I. Yarita, H. Abe, T. Mikuriya, and F. Yanagishima, "Technologies of flying gauge change in fully continuous cold rolling mill for thin gauge steel strips," *IRSID Rolling Conf*, vol. 2, 1987, pp. E.36.1-E.36.11.
- [2] J. S. Wang, Z. Y. Jiang, A. K. Tieu, X. H. Liu, and G. D. Wang, "A flying gauge change model in tandem cold strip mill," *Journal of materials processing technology*, vol. 204, Issues 1-3, Aug. 2008, pp. 152-161.
- [3] C. W. J. Hol, S. Sujoto, M. de Boer, V. Beentjes, M. Price, C. W. Scherer, and A. A. J. van der Winden, "Optimal Feedforward Filter Design for Flying Gauge Changes of a Continuous Cold Mill," *IFAC World Congress*, vol. 18, Aug. 2011, pp. 8545-8551.
- [4] D. R. Bland and H. Ford, "The Calculation of Roll Force and Torque in Cold Strip Rolling with Tensions," *Proceedings of the Institution of Mechanical Engineers*, vol. 159, Jun. 1948, pp. 144-163.
- [5] R. Hill, *The Mathematical Theory of Plasticity*. Oxford University Press, Aug. 1998.